

# First Studies of Pure Electron Plasmas in the Columbia Non-neutral Torus

J.W. Berkery\*, T.S. Pedersen\*, J.P. Kremer\*, R.G. Lefrancois\*, Q.R. Marksteiner\*, A.H. Boozer\*, H. E. Mynick†, N. Pomphrey†, W. Reiersen†, F. Dahlgreen†, H. Himura\*\* and X. Sarasola‡

\*Dept. of Applied Physics and Applied Mathematics, Columbia University, New York, NY 10027

†Princeton Plasma Physics Laboratory, Princeton, NJ 08543

\*\*Kyoto Institute of Technology, Kyoto, Japan

‡CIEMAT, Madrid, Spain

**Abstract.** The first studies of pure electron plasmas confined on magnetic surfaces in the Columbia Non-neutral Torus are overviewed. The electron plasma is created by a thermionic emitter filament and similar filaments mounted on ceramic rods are used as Langmuir and emissive probes. The equilibrium density, temperature and potential profiles are experimentally measured. Numerical calculations of the equilibrium agree well with measurements and also predict a toroidal density variation of a factor of four. The confinement time is found to decrease with increased neutral pressure and emitter bias voltage, and it is presently limited to 20 ms by the insulated emitter and probe rods. A retractable electron emitter and external diagnostics will be used to determine the confinement time in the absence of rods. Ion driven instabilities are observed at high neutral pressure and low magnetic field strength. Further research of these instabilities will be carried out.

PACS: 52.27.Jt, 52.55.Hc, 52.27.Aj

## INTRODUCTION

Non-neutral plasmas have been mostly studied in Penning-Malmberg traps [1, 2] and pure toroidal traps [3, 4, 5]. When produced on nested magnetic surfaces, however, these plasmas have some characteristics that are desirable for fusion applications. The high electric fields in non-neutral plasmas can result in large  $E \times B$  drifts within magnetic surfaces that can greatly improve the confinement time of the plasma [6]. Non-neutral plasmas confined on magnetic surfaces have not been previously studied, and the equilibrium and transport properties are fundamentally different from previously studied configurations [7, 8, 9, 10]. The behavior of such plasmas can be addressed by studying pure electron plasmas in the Columbia Non-neutral Torus.

The Columbia Non-neutral Torus (CNT) [11] is a stellarator in which the nested magnetic surfaces are created from only four circular coils (see figure 1). The average major radius is 0.28 m and the average minor radius is 0.15 m. The aspect ratio of less than 1.9 is the lowest ever achieved in a stellarator. CNT can operate at steady state with  $B < 0.06$  Tesla.

The major research questions of CNT that are addressed in this paper are as follows. First, does a pure electron plasma have a stable equilibrium in a stellarator? Theory predicts that stable equilibria do exist [7]. Both experimental [12] and numerical [10] characterizations of this equilibrium have been carried out.

**FIGURE 1.** A cutaway CAD drawing of the Columbia Non-neutral Torus is shown (left). Included are the vacuum vessel (cut in half), the two outer poloidal field coils, the two inner interlocking coils, and a rendering of the last closed magnetic flux surface. On the right a rendering of the nested magnetic surfaces is shown.

Second, can confinement in such a device be excellent - seconds, even minutes or hours? Confinement in CNT is predicted to be limited by neoclassical effects [7], and stellarator neoclassical transport in the presence of a non-negligible electric field scales like  $\tau_c \sim (e\Phi/T)^2/v$ . Small Debye length pure electron plasmas have  $(e\Phi/T)^2 \sim (a/\lambda_D)^4 \gg 1$  and therefore extremely long confinement is predicted. Experimental investigations of the confinement are discussed.

Finally, what are the properties of the partially neutralized plasmas that can be created in a stellarator? In particular, observations of ion driven instabilities are discussed and plans for further investigation are presented.

## CREATION OF PURE ELECTRON PLASMAS

The first step towards the creation of a pure electron plasma in magnetic surfaces is to verify the magnetic topology of the device. This has been accomplished using the fluorescent rod method of field line mapping [13]. Excellent quality nested magnetic surfaces have been verified and they match well with predictions from numerical calculations.

Secondly, the electrons must be introduced into the magnetic surfaces. The electron source employed in CNT is thermionic emission from a heated tungsten filament placed on the magnetic axis. The filament is biased negatively, but has no anode, unlike an e-gun. Parallel transport fills the field line on axis in about  $1 \mu\text{s}$ . Perpendicular transport fills the rest of the surfaces and finally a steady state is reached between emission and radial losses. Presently, CNT uses two ceramic rods with arrays of filaments. The filaments are halogen light bulbs (without the bulb glass), and each filament can serve multiple functions: electron emitter, Langmuir probe, or emissive probe.

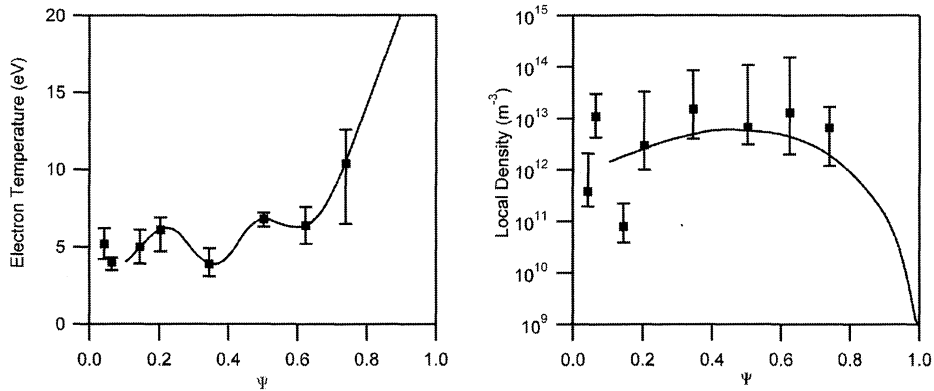


**FIGURE 2.** Measured temperature (left) and density (right) profiles measured with a Langmuir probe array in a pure electron plasma with magnetic field of 0.02 Tesla, neutral pressure of  $2 \times 10^{-8}$  Torr, and electron emitter bias of -300 V. The curve fits are used as inputs to the equilibrium reconstruction code.

## EQUILIBRIUM

### Measured equilibrium profiles

Temperature, density and potential measurements with probes are complicated by the large Debye lengths (compared to the probe size), low temperatures, low densities and high potentials of pure electron plasmas [14]. Such measurements are possible, using Langmuir probes (cold) and emissive probes (hot), although the measurement of density, in particular, has a relatively large error [12].

In CNT an array of eight probes mounted on a ceramic rod are used to measure profiles of temperature and density. Each probe is a small coil of tungsten wire from a halogen light bulb. The local plasma potential is measured as the deviation potential – the potential where the emissive probe I-V curve deviates from the Langmuir probe I-V curve [14, 15]. The temperature is measured in the conventional way, from the Langmuir probe I-V curve. The electron density can be obtained from this curve as well, with knowledge of the local potential.

With the conditions of 0.02 Tesla magnetic field,  $2 \times 10^{-8}$  Torr neutral pressure and -300 V emitter bias, the interior temperature is seen to be about 5 eV (figure 2). The measured density profile is also shown in figure 2. Together these measurements show that the Debye length is about 1.5 cm, which is much less than the minor radius of CNT, so the plasma criterion is satisfied. Profiles such as these have been obtained for a wide variety of conditions, including a range of magnetic field strengths, neutral pressures, and emitter biases (for another example, and for more details on the measurements, see reference [12]).

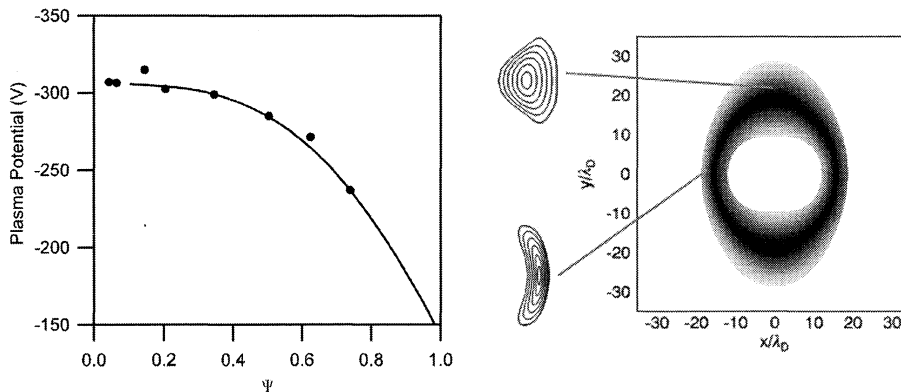


**FIGURE 3.** The potential profile for the conditions of figure 2 is shown on the left. The measurements are compared to the calculated potential profile from the equilibrium reconstruction code. On the right, the variation of the calculated potential through the changing cross sections is demonstrated (darker areas corresponding to larger negative potentials). The locations of the thin and fat cross sections are indicated by Poincaré maps of their magnetic surfaces.

### Equilibrium reconstruction

The equilibrium of a pure electron plasma confined on magnetic surfaces is characterized by the potential, density and temperature profiles. A non-linear equation for the potential can be written in terms of the density and temperature as functions of  $\Psi$ , the magnetic flux coordinate [7],

$$\nabla^2 \Phi = \frac{e}{\epsilon_0} N(\Psi) \exp\left(\frac{e\Phi}{T_e(\Psi)}\right). \quad (1)$$

Here, electron number density profile is given by  $N(\Psi)$  times the exponential term.

A fully 3-D code has been developed to solve the equilibrium equation for arbitrary boundary conditions [10]. Measured density and temperature profiles, shown in figure 2, then allow a complete CNT equilibrium reconstruction. The measured potential profile shows good agreement with the potential profile obtained by solving equation 1 with the 3-D code (figure 3).

### Predicted Toroidal Density Variation

One consequence of the changing cross-sectional area of the plasma in CNT that is predicted by the calculation is a large toroidal density variation. While the potential is roughly constant along field lines, the density is higher at smaller cross-sections (like in a Penning-Malmberg or min-B trap [16]). The calculation for a  $\lambda_D = 1.5$  cm plasma, predicts a factor of about four variation of density on the magnetic axis. This is illustrated graphically in figure 4. Installation of new probes with the ability to sweep through a

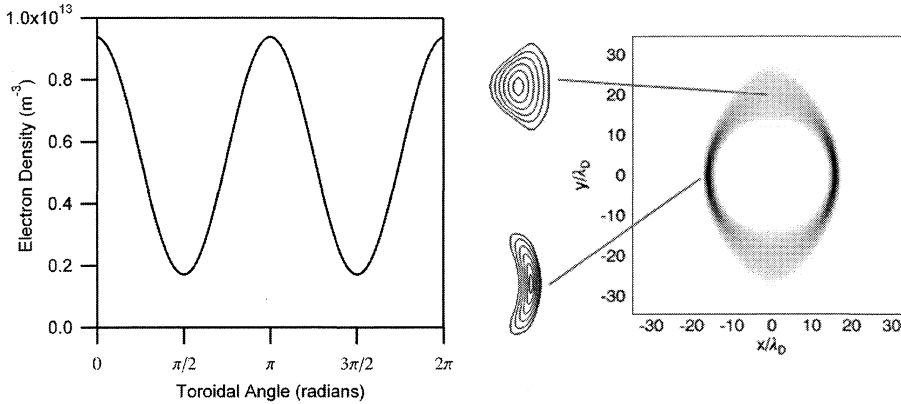


**FIGURE 4.** A sinusoidal curve fit of the calculated electron density on the magnetic axis vs. the toroidal angle for the conditions of figure 2 is shown on the left. The density is predicted to vary by a factor of five. On the right, this variation is displayed schematically, showing that the high density region (dark) is located at the thin cross section.

cross section will allow for simultaneous measurement of equilibrium profiles in the two principal cross sections. By making direct density profile measurements, the prediction of the calculation can be verified.

## CONFINEMENT

Knowing the electron source rate, and the total electron inventory, the confinement time can be computed as  $\tau_c \approx eN/I_e$ . The source rate,  $I_e$ , is measured from the steady-state emission current of the electron emitter. The total electron inventory,  $N$ , is known from the volume averaged density obtained through density profile measurements (figure 2). Confinement times up to 20 ms have been measured.

The parallel force balance within a magnetic surface establishes itself in about  $10 \mu\text{s}$ , so the electron fluid is in flux surface equilibrium. Also, there are no large scale cross-surface  $E \times B$  flows, as these would lead to particle losses in  $10 - 100 \mu\text{s}$ . Finally, there are no significant direct bad orbit losses since direct  $\nabla B$  drift out of the device would occur in about  $300 \mu\text{s}$ . Therefore the plasma is in a macroscopically stable equilibrium. With a theoretical confinement time scaling of  $\tau_c \approx \tau_{ee}(a/\lambda_D)^4$  [17], and values of electron-electron collision time of  $\tau_{ee} \approx 10^{-3}\text{s}$  and minor radius to Debye length ratio of about 10 in CNT, confinement times on the order of 10 seconds may be expected. In this case, the question must be asked: what limits the confinement?

It has been found that the insulated rods that hold the emitter and probes limit the confinement [12]. When two rods are used, they give twice as much transport as one rod (see figure 5). The rods are insulating, so they are not steady state sinks for electrons, but instead they act as large electrostatic perturbations that drives  $E \times B$  transport. This happens when the insulated rods charge up negative relative to plasma and the resulting  $E \times B$  drift pattern convects particles along the rod all the way to the open

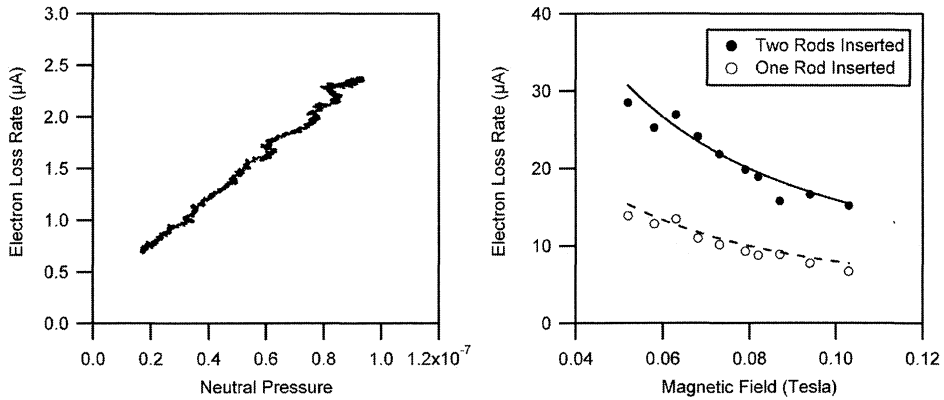


**FIGURE 5.** The trend of confinement with neutral pressure (left) and magnetic field strength (right) are displayed. For the left graph the emitter bias was -200 and the magnetic field was 0.1 Tesla. For the right graph the emitter bias was -400 and the neutral pressure was  $6.7 \times 10^{-9}$  Torr. The data in the left plot was taken continuously (in one shot) as the pressure was raised.

field lines. The observed  $1/B$  scaling of the transport rate is consistent with this effect. In figure 5 the curve fits shown are  $(1.6\mu A/Tesla)/B$  for the case of two rods inserted and  $(0.8\mu A/Tesla)/B$  for one rod. The issue of rod-limited confinement can be avoided by retracting the electron emitter and by using external probes, as described in the next subsections.

Despite the present limitation on the confinement time, information about its scaling can be experimentally obtained. The steady-state emission current, which is equal to the electron loss rate and inversely proportional to the confinement time, assuming an approximately constant total electron inventory between conditions, is plotted in figure 5 vs. neutral pressure and vs. magnetic field strength. The latter dependency has been explained above. The dependency of confinement time on neutral pressure can not be explained in a classical sense, because the electron-neutral collision rate is small enough in CNT that it cannot explain the amount of transport seen. Investigations of the dependencies of confinement time on neutral pressure are ongoing.

### Retractable emitter

A retractable electron emitter is desired to remove the perturbing effect of the ceramic rods from the plasma, so an unperturbed confinement time can be measured. To accomplish this, the emitter must be able to retract from the magnetic axis to the last closed flux surface in 20 ms, while filling the surfaces with electrons. A pneumatic system has been constructed that meets these goals. The system consists of a filament on the end of an insulated rod that is connected, through a vacuum bellows to a pneumatic piston. The filament is positioned on the on the far side of the magnetic axis and the motion is initiated when a solenoid valve switches gas in a high pressure reservoir to the piston. The

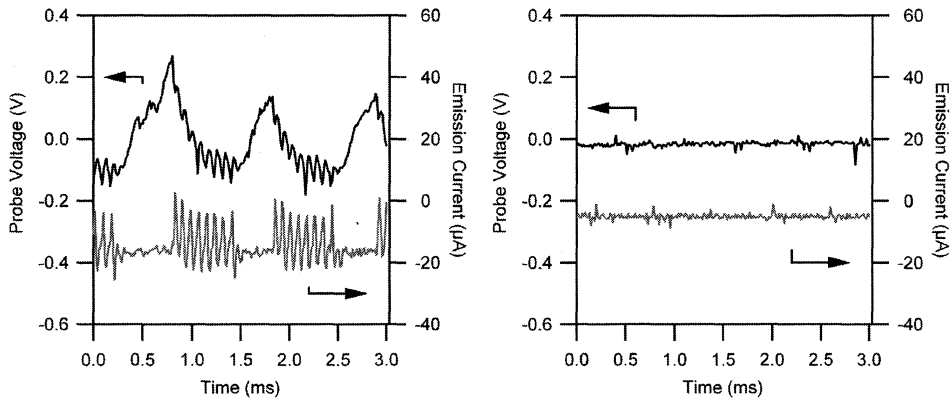


**FIGURE 6.** Plots showing the ion driven instability as seen on a floating emissive probe voltage signal and the emission current signal vs. time. In both cases the magnetic field was 0.02 Tesla and the emitter bias was  $-200$  Volts. On the left plot, the neutral pressure was  $2 \times 10^{-7}$  Torr, while on the right plot it was  $2.2 \times 10^{-8}$  Torr.

filament then speeds up, moves through the surfaces from the axis to the last closed flux surface with a high velocity, and is then decelerated by shock absorbers. By utilizing the thin cross section of the magnetic geometry in CNT, the filament can move through the plasma in about 20 ms. This system is fully constructed and installed, and is currently being tested.

## Capacitive probes

In addition to a non-perturbing method of creating the plasma, a non-perturbing method of diagnosing the plasma is required to measure the unperturbed confinement time. Sector probes have been employed in various non-neutral plasma experiments to diagnose the plasma [18, 19]. Sector probes are conducting surfaces that conform to the outside surface of the plasma volume. The total surface area is broken into a number of distinct sectors, each of which is individually biased or floated. The image charge of the plasma is then measured on the probes. The decay of the image charge can be used as a diagnostic of the confinement time. A set of 10 sector probes has been constructed. They will be used in CNT to diagnose the plasma in a unperturbing manner.

## ION DRIVEN INSTABILITIES

At the low neutral pressures achieved in CNT ( $5 \times 10^{-9} - 1 \times 10^{-8}$  Torr), the ion content has been measured with a large ion-collecting probe inserted in the plasma to be less than one percent. Thus, the plasmas in CNT can be considered pure electron plasmas. If there was no sink for the ions, they would continue to accumulate, which they do not. This steady state occurs because the insulated emitter and probe rods act as sinks

for the ions after they charge up negatively. When the plasma is created and diagnosed in a non-perturbing manner, the expected buildup of ions may be a limiting factor for confinement.

At much higher neutral pressures ( $\approx 2 \times 10^{-7}$  Torr), the plasma in CNT contains 4 – 10% ions. At relatively low magnetic field strength this can trigger instabilities, similar to what has been observed in the CHS stellarator [20]. The observed oscillations are in the 10 – 25 kHz range.

Figure 6 shows the ion driven oscillations as observed with a floating emissive probe and on the emission current signal, while the neutral pressure was  $2 \times 10^{-7}$  Torr and the magnetic field was 0.02 Tesla. When the neutral pressure was decreased by an order of magnitude, the decrease in the ion content causes the steady-state emission current to decrease because the confinement has improved, and the oscillations are suppressed.

In the first graph of figure 6, a 12 kHz oscillation is seen, which seems to come in  $\sim 0.6$  ms bursts, and then disappear for  $\sim 0.4$  ms. As the neutral pressure is raised even higher, the bursts become longer and the time in between them becomes shorter, until at  $2.2 \times 10^{-7}$  torr, the 12 kHz oscillations are continuous. The quiescent periods between bursts suggest that for low enough neutral pressure, the instability itself can reduce the ion content of the plasma enough to make the plasma temporarily stable. This may come about because the instability takes energy from the ions, bringing them closer to the magnetic axis and making them more likely to collide with one of the insulating rods.

Further work is planned to understand these oscillations. Planned experiments include introducing ions of various species into the plasma to observe the effect of ion mass and measuring the spatial structures of the oscillations using new probes and electronics. The oscillations will also be compared with theories and observations of ion driven instabilities in other confinement devices [21, 22, 23].

## CONCLUSIONS

Pure electron plasmas confined on magnetic surfaces have been studied in the Columbia Non-neutral Torus. Equilibrium density, temperature and potential profiles were measured using Langmuir and emissive probes. The density and temperature profiles are used as inputs to an equilibrium reconstruction code that then accurately matches the potential profile. This code also predicts a toroidal density variation of a factor of four. This prediction will be experimentally verified with a new cross-section sweeping probe. Measured confinement times were limited to 20 ms by the electrostatically perturbing presence of the insulating probe rods, however, the confinement time was found to decrease with increasing neutral pressure and increasing emitter bias voltage. The unperturbed confinement time will be measured with a retractable emitter and external sector probes. Observations from high neutral pressure and low magnetic field strength experiments indicate that a buildup of ions in the electron plasma can lead to ion driven instabilities. Further research of these instabilities is planned.

## ACKNOWLEDGMENTS

This work is supported by the United States DOE Grant DE-FG02-02ER54690, the NSF-DOE Partnership in Basic Plasma Science, Grant NSF-PHY-04-49813, the NSF CAREER program, Grant NSF-PHY-04-49813, and the DOE Fusion Energy Sciences Postdoctoral Research Program.

## REFERENCES

1. R. Davidson, *Physics of Nonneutral Plasmas*, Imperial College Press and World Scientific Publishing, London, UK, 2001.
2. J. Malmberg, and J. deGrassie, *Physical Review Letters* **35**, 577–580 (1975).
3. J. Daugherty, J. Eninger, and G. Janes, *Physics of Fluids* **12**, 2677–2693 (1969).
4. P. Zaveri, P. John, K. Avinash, and P. Kaw, *Physical Review Letters* **68**, 3295–3298 (1992).
5. M. Stoneking, M. Growdon, M. Milne, and R. Peterson, *Physical Review Letters* **92** (2004).
6. T. S. Pedersen, *New Developments in Nuclear Fusion Research*, Nova Publishers, 2006, chap. Large Electric Fields in Stellarators, pp. 0–0.
7. T. S. Pedersen, and A. Boozer, *Physical Review Letters* **88**, 205002 (2002).
8. A. Boozer, *Physics of Plasmas* **12**, 034502 (2005).
9. A. Boozer, *Physics of Plasmas* **12**, 104502 (2005).
10. R. Lefrancois, T. S. Pedersen, A. Boozer, and J. Kremer, *Physics of Plasmas* **12**, 072105 (2005).
11. T. S. Pedersen, A. Boozer, J. Kremer, R. Lefrancois, W. Reiersen, F. Dahlgreen, and N. Pomphrey, *Fusion Science and Technology* **46**, 200–208 (2004).
12. J. Kremer, T. S. Pedersen, Q. Marksteiner, and R. Lefrancois, *Physical Review Letters* (2006), accepted for publication.
13. T. S. Pedersen, J. Kremer, R. Lefrancois, Q. Marksteiner, X. Sarasola, and N. Ahmad, *Physics of Plasmas* **13**, 012502 (2006).
14. J. Kremer, T. S. Pedersen, Q. Marksteiner, and R. Lefrancois, (*submitted to Review of Scientific Instruments*) (2006).
15. M. Cho, C. Chan, N. Hershkowitz, and T. Intrator, *Review of Scientific Instruments* **55**, 631–632 (1984).
16. J. Fajans, *Physics of Plasmas* **10**, 1209–1214 (2003).
17. T. S. Pedersen, A. Boozer, J. Kremer, and R. Lefrancois, *Physics of Plasmas* **11**, 2377–2381 (2004).
18. R. Greaves, M. Tinkle, and C. Surko, *Physical Review Letters* **74**, 90–93 (1995).
19. H. Higaki, and A. Mohri, *Physics Letters A* **235**, 504–507 (1997).
20. H. Himura, H. Wakabayashi, M. Fukao, M. Isobe, S. Okamura, and H. Yamada, *IEEE Transactions on Plasma Science* **32**, 510–516 (2004).
21. R. Levy, J. Daugherty, and O. Buneman, *Physics of Fluids* **12**, 2616–2629 (1969).
22. A. Peurrung, J. Notte, and J. Fajans, *Physical Review Letters* **70**, 295–298 (1993).
23. M. Stoneking, P. Fontana, R. Sampson, and D. Thuecks, *Physics of Plasmas* **9**, 766–771 (2002).